

Synthesis and properties of *a*-axis and *b*-axis oriented $\text{GdBa}_2\text{Cu}_3\text{O}_{7-\delta}$ high T_c thin films

O. Nakamura,^{a)} J. Guimpel,^{b)} F. Sharifi, R. C. Dynes, and Ivan K. Schuller
Physics Department-0319, University of California, San Diego, La Jolla, California 92093-0319

(Received 23 April 1992; accepted for publication 18 September 1992)

We report the growth and properties of *a*-axis oriented $\text{GdBa}_2\text{Cu}_3\text{O}_{7-\delta}$ high T_c thin films on (100) SrTiO_3 substrates by dc magnetron sputtering. It is found that $\text{GdBa}_2\text{Cu}_3\text{O}_{7-\delta}$ films on (100) SrTiO_3 exhibit *a*-oriented growth at higher substrate temperatures compared with $\text{YBa}_2\text{Cu}_3\text{O}_{7-\delta}$ films. By utilizing low-temperature-grown *a*-axis $\text{GdBa}_2\text{Cu}_3\text{O}_{7-\delta}$ films (200 Å in thickness) as a self-template, pure *a*-axis films can be grown at elevated temperatures. The growth of *b*-axis film on vicinal (100) SrTiO_3 under similar growth conditions is also reported.

Non-*c*-axis-oriented 123 high T_c thin films may be advantageous for applications in tunneling and Josephson devices because of the substantially longer superconducting coherence length ξ_0 in the planes (12–15 Å) than along the *c*-axis (2–3 Å) (GBCO). Among the variety of non-*c*-oriented films reported to date,^{1–4} *in situ a*-oriented $\text{YBa}_2\text{Cu}_3\text{O}_{7-\delta}$ -YBCO films appear attractive because of the very smooth surfaces produced.⁵ It is well established that YBCO and related materials, such as $\text{EuBa}_2\text{Cu}_3\text{O}_{7-\delta}$ exhibit *a*-oriented growth on lattice constant matched substrates, e.g., SrTiO_3 (STO) and LaAlO_3 , at reduced substrate temperatures.^{4–7} These low-temperature-grown *a*-oriented films show a suppressed superconducting transition temperature, T_c of 80–85 K, probably due to disorder in the films, inherent to low-temperature growth. One possible approach to obtain higher quality *in situ a*-axis films is to develop a growth technique at higher substrate temperatures (T_s). Inam *et al.*⁸ used an *a*-axis $\text{PrBa}_2\text{Cu}_3\text{O}_{7-\delta}$ film as a template followed by the deposition of an *a*-axis YBCO film at higher T_s . They observed a high T_c onset of 92 K and smooth surfaces although these were grown at high temperature. *a*-axis growth of YBCO at higher T_s , where *c*-axis orientation usually is found, suggests that other factors in addition to the usual lattice matching play an important role. Earlier,⁹ we have found that $\text{DyBa}_2\text{Cu}_3\text{O}_{7-\delta}$ grows (110) oriented on (110) $\text{LaBa}_2\text{Cu}_3\text{O}_y$ at substrate temperatures up to 700 °C.

In this letter, we report the growth and properties at *a*-axis oriented $\text{GdBa}_2\text{Cu}_3\text{O}_{7-\delta}$ (GBCO) high T_c thin films on (100) STO substrates by dc magnetron sputtering. By utilizing low-temperature-grown *a*-axis GBCO films (200 Å in thickness) as a self-template, pure *a*-axis films can be grown at elevated temperatures higher than those used usually for $\text{YBa}_2\text{Cu}_3\text{O}_{7-\delta}$. The growth of *b*-axis film on vicinal (100) STO under similar growth conditions is also reported.

The details of the fabrication technique have been previously described.¹⁰ We use here two methods to prepare *a*-axis GBCO films. First, a set of films are grown at dif-

ferent T_s to determine the epitaxial behavior versus T_s . Next, we investigate a two-step- T_s deposition, in which the first 10% of the total thickness of a film is grown at lower T_s [≈ 600 °C] at which GBCO film shows perfect *a*-axis growth, and then T_s is increased to the final value. The deposition of the film is uninterrupted while T_s is increased. The film thickness deposited during this transition period is 5%–10% of the total film thickness of ≈ 2000 Å. The orientation of the films are studied by θ -2 θ x-ray diffraction (XRD) using $\text{CuK}\alpha$ radiation. The mosaic spread of the *a*-axis grains is measured from the θ (rocking curve) scan along its (200) reflection. The volume percent of the *a*-axis oriented sample is estimated from the (005) and (200) reflection intensities and their FWHMs of both θ -2 θ and θ scans. The superconducting transition temperature T_c is measured by the conventional four-probe resistive dc method. T_s quoted in this study is the estimated substrate temperature, which is calibrated using a secondary thermocouple in different runs, and is ≈ 100 °C lower than the substrate carrier temperature.

Figure 1 shows the *a*-axis volume percent, the mosaic spread of *a*-axis domains, and the T_c 's of the films. For the two-step- T_s films, the final T_s is shown in the figure and the results for YBCO films are included for comparison. Although YBCO films studied here (≈ 900 Å in thickness) are thinner than GBCO films (≈ 2000 Å), comparison is possible since we found the film properties to be only slightly affected by thickness in this range. It is clear from Fig. 1 that GBCO exhibits *a*-oriented growth with a narrow mosaic spread of 0.07° – 0.08° (instrumental broadening $\sim 0.03^\circ$) at higher T_s than YBCO. This could be explained by the better lattice constant match of GBCO than YBCO¹¹ with STO¹² (the bulk lattice constants are STO; $a=3.90$ Å, YBCO; $a=3.82$ Å, $b=3.88$ Å, $c/3=3.89$ Å, GBCO; $a=3.84$ Å, $b=c/3=3.90$ Å). The films grown at lower temperatures show a depressed T_c , perhaps due to disorder which is not resolved by the x-ray diffraction method.^{13,14}

With the constant- T_s method, the best result for GBCO films (*a* volume $\approx 100\%$, midpoint transition temperature $T_c=86.4$ K, 90% to 10% transition width $\Delta T_c=5.4$ K) is obtained at $T_s=640$ °C, which is 80 °C higher than the optimal T_s for YBCO. By applying the two-step- T_s method, we found the T_s can be further increased. It

^{a)}On leave from the Corporate Research and Development Laboratory, Tonen Corporation, 1-3-1 Nishi-Tsurugaoka, Ohi-Machi, Saitama 354, Japan.

^{b)}On leave from the Centro Atomico Bariloche, 8400 S.C. de Bariloche, Rio Negro, Argentina.

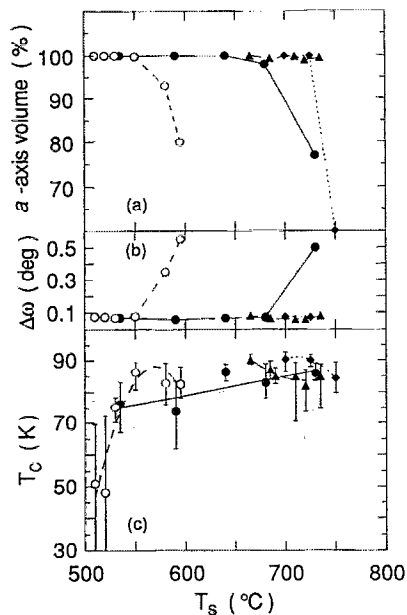


FIG. 1. (a) a -axis volume percent, (b) a -axis grains mosaic spread [FWHM of the rocking curve scan along the (200) peak], and (c) T_c as a function of substrate temperature, T_s , for $\text{YBa}_2\text{Cu}_3\text{O}_{7-\delta}$ and $\text{GdBa}_2\text{Cu}_3\text{O}_{7-\delta}$ films. In (c), the symbol denotes the midpoint T_c and error bars show the 90% to 10% resistive transition widths. Open circles; $\text{YBa}_2\text{Cu}_3\text{O}_{7-\delta}$ films ($\approx 900 \text{ \AA}$), solid circles; $\text{GdBa}_2\text{Cu}_3\text{O}_{7-\delta}$ films, solid diamonds; $\text{GdBa}_2\text{Cu}_3\text{O}_{7-\delta}$ films by the two-step- T_s method, solid triangles; $\text{GdBa}_2\text{Cu}_3\text{O}_{7-\delta}$ films by the two-step- T_s method from the 1:2.05:3.10 composition target. All $\text{GdBa}_2\text{Cu}_3\text{O}_{7-\delta}$ films are of $\approx 2000 \text{ \AA}$ in total thickness. Some data points are shifted 5 K along the temperature axis for clarity of display. The lines are guides to the eye.

was reported earlier¹⁵ that the a -axis oriented growth of YBCO is very sensitive to cation composition of the sputtering targets and that copper-rich targets together with low substrate temperatures are necessary for the successful growth of a -axis YBCO films on STO and LaAlO_3 . We have also found the a -axis film properties to be very sensitive to small changes in the target composition. A slightly barium and copper rich target gives the optimal $T_s \approx 670 \text{ }^\circ\text{C}$ while the stoichiometric target gives the best result at $\approx 730 \text{ }^\circ\text{C}$. In both cases, however, a midpoint T_c larger than 90 K with $\Delta T_c \approx 3 \text{ K}$ can be obtained by the two-step- T_s method. For c -axis films, slight changes in target composition result in almost negligible changes in film properties.

Figure 2 shows a representative θ - 2θ XRD spectra of a - and c -axis films. The figure includes the XRD spectra of a b -axis film grown on (100) SrTiO_3 18° faceted towards the [010] direction obtained by the two-step- T_s method with the final $T_s \approx 750 \text{ }^\circ\text{C}$. The XRD spectra taken in the standard θ - 2θ geometry with the beam and detector in the plane formed by the [100] and [010] STO axes only allows access to a restricted angular range $2\theta > 36^\circ$ in Fig. 2(b). We identify this film as b -axis oriented from the following characteristics; (1) No (100) reflection is observed in the XRD spectra and (00 n) reflections are much weaker for a c -axis film. (2) The STO (200) reflection has θ scan FWHM of 0.08° , wider than the 0.03° for the same reflection from the bare substrate without GBCO film. This in-

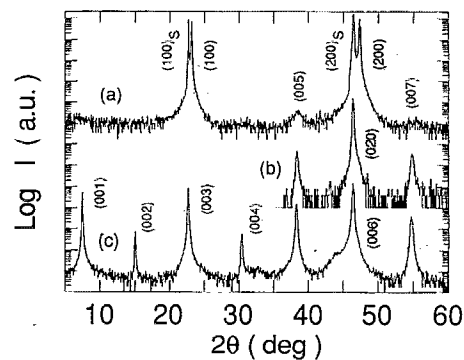


FIG. 2. Representative θ - 2θ XRD spectra for a -, b -, and c -axis $\text{GdBa}_2\text{Cu}_3\text{O}_{7-\delta}$ films on (100) SrTiO_3 , b -axis film was grown on 18° faceted (100) SrTiO_3 and XRD spectra were taken around the [100] SrTiO_3 direction. Indexing in the figure for $\text{GdBa}_2\text{Cu}_3\text{O}_{7-\delta}$ films; (100)_s and (200)_s denote SrTiO_3 reflections.

dicates an overlap from the GBCO (020) reflection. (3) Normal state resistivity of the film (Fig. 3) is of the same order as a -axis film and much higher than c -axis film. To estimate the volume fraction of c -axis crystals, the (007) GBCO peak intensity and FWHM of θ - 2θ and θ scans are measured in both the b - and c -axis films. By comparing the normalized (007) reflection intensities we estimate the b -axis volume percent to be at least 90%. In this film, the b axis of GBCO is parallel to the [100] STO direction, at 18° to the substrate normal. The final a or b orientation of the films is determined during the low-temperature oxygen soaking procedure, since GBCO is tetragonal at the deposition condition.¹⁶ On the vicinal STO, a better lattice match is obtained between the GBCO b axis and the (010) STO plane, which may favor the growth of b -axis films.

Representative resistivity versus temperature curves are shown in Fig. 3. a - and b -axis films have ≈ 10 times higher resistivity at room temperature than similar c -axis films, which may be explained by the dense 90° grain boundaries found in *in situ* a -axis films.^{5,8} A semiconductor-like $\rho(T)$ behavior of a -axis films was found earlier in the literature.⁴ Although metallic behavior⁵⁻⁸ is usually reported, we found that $\rho(300 \text{ K})/\rho(100 \text{ K})$, which characterizes the metallicity of the sample, decreases with decreasing final T_s in the two-step-grown

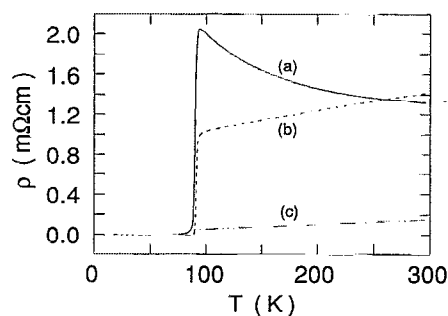


FIG. 3. Resistivity vs temperature curves of $\text{GdBa}_2\text{Cu}_3\text{O}_{7-\delta}$ films with (a) a - oriented by the two-step- T_s method, (b) b -axis oriented by the two-step- T_s method, and (c) typical c -axis oriented film.

films. We note that *a*-axis YBCO and GBCO films grown by the constant- T_s method at lower temperature exhibit a positive slope in resistivity; however, $\rho(300\text{ K})$ are similar to the two-step films in Fig. 1. Our optimized *a*-axis films grown by the two-step method show relatively sharp 90% to 10% transitions but often exhibit a small resistivity tail to lower temperature; typical zero-resistance T_c is 80–85 K. Note that the *b*-axis film shows a sharp superconducting transition of $\Delta T_c \approx 2\text{ K}$ and zero-resistance $T_c > 89\text{ K}$.

This behavior suggests the possibility of crack formation in *a*-axis films, like in (110)¹⁷ oriented films where the cracks increase with increasing T_s . In spite of this speculation, we find that our *a*-axis films exhibit very smooth, featureless surfaces under optical and scanning electron microscope inspection down to a resolution of 50 Å before and after light bromine etch. It is not clear, therefore, why the *b*-axis films show metallic behavior, whereas *a*-axis films grown under almost identical conditions exhibit semi-conducting characteristics.

For *a*-axis films, the properties degrade with increasing T_s above the optimal temperature. We expect that the inclusions of *c*-axis growth caused by higher T_s would not reduce T_c . We are left, therefore, to conclude that crack formation caused at higher T_s by the differential thermal contraction together with the stresses caused by the mixture of the *a* and *c* axis, may explain the T_c degradation. Further indirect evidence for crack formation is also provided by independent tunneling measurements presently under investigation.

In conclusion, we have grown *a*- and *b*-axis oriented GBCO and YBCO films at moderately elevated temperatures, on self-templates grown at lower temperatures. X-ray and transport measurements show them to be of high quality. There are some indications of crack formation in the *a*-axis films.

The authors thank S. L. Bud'ko for useful discussions

and pressure experiments and I. N. Chan for preparing YBCO targets. One of us, J. G., acknowledges CONICET, Argentina for providing some international travel funding through a fellowship. This work was supported by the ONR Grant No. N00014-88K-0480. We thank Professor K. Kitazawa and Dr. T. Izumi for arranging the Tonen-UCSD collaboration.

- ¹Y. Enomoto, T. Murakami, M. Suzuki, and K. Moriwaki, *Jpn. J. Appl. Phys.* **26**, L1248 (1987).
- ²J. Fujita, T. Yoshitake, A. Kamijo, T. Satoh, and H. Igarashi, *J. Appl. Phys.* **64**, 1292 (1988).
- ³T. Terashima, Y. Bando, K. Iijima, K. Yamamoto, and K. Hirata, *Appl. Phys. Lett.* **53**, 2232 (1988).
- ⁴G. Linker, X. X. Xi, O. Meyer, Q. Li, and J. Geerk, *Solid State Commun.* **69**, 249 (1989).
- ⁵C. B. Eom, A. F. Marshall, S. S. Laderman, R. L. Jacowitz, and T. H. Geballe, *Science* **249**, 1549 (1990).
- ⁶H. Asano, M. Asahi, and O. Michikami, *Jpn. J. Appl. Phys.* **28**, L981 (1989).
- ⁷G. C. Xiong and S. Z. Wang, *Appl. Phys. Lett.* **55**, 902 (1989).
- ⁸A. Inam, C. T. Rogers, R. Ramesh, K. Remschnig, L. Farrow, D. Hart, T. Venkatesan, and B. Wilkens, *Appl. Phys. Lett.* **57**, 2484 (1990).
- ⁹O. Nakamura, I. Chan, J. Guimpel, and I. K. Schuller, *Appl. Phys. Lett.* **59**, 1245 (1991).
- ¹⁰O. Nakamura, E. E. Fullerton, J. Guimpel, and I. K. Schuller, *Appl. Phys. Lett.* **60**, 120 (1992).
- ¹¹A. A. R. Fernandes, J. Santamaria, S. L. Bud'ko, O. Nakamura, J. Guimpel, and I. K. Schuller, *Phys. Rev. B* **44**, 7601 (1991).
- ¹²F. S. Galasso, *Structure and Properties of Inorganic Solids* (Pergamon, New York, 1970).
- ¹³K. Shinohara, V. Matijasevic, P. A. Rosenthal, A. F. Marshall, R. H. Hammond, and M. R. Beasley, *Appl. Phys. Lett.* **58**, 756 (1991).
- ¹⁴E. Sodtke and H. Münder, *Appl. Phys. Lett.* **60**, 1630 (1992).
- ¹⁵C. B. Eom, J. Z. Sun, B. M. Lairson, S. K. Streiffer, A. F. Marshall, K. Yamamoto, S. M. Anlage, J. C. Bravman, and T. H. Geballe, *Physica C* **171**, 354 (1990).
- ¹⁶J. Jorgensen, M. A. Beno, D. G. Hinks, L. Soderholm, K. H. Volin, R. L. Hitterman, J. D. Grace, I. K. Schuller, C. U. Segre, K. Zhang, and M. S. Kleefish, *Phys. Rev. B* **36**, 3608 (1987).
- ¹⁷E. Olsson, A. Gupta, M. D. Thouless, A. Segmüller, and D. R. Clarke, *Appl. Phys. Lett.* **58**, 1682 (1991).